Synthesis of carbon nanoparticles from $Ar/H_2/C_2H_2$ plasmas: analysis of the film properties and electron energy distribution function

M. Camero[1], F. J. Gordillo-Vázquez[2], C. Gómez-Aleixandre[1]

[1]*Instituto de Ciencia de Materiales de Madrid, CSIC, 28049 Cantoblanco, Madrid, Spain*
[2] *Instituto de Óptica, CSIC, Serrano 121, 28006 Madrid, Spain*

A study of the synthesis of carbon nanoparticles embedded in carbon thin films deposited by radiofrequency (13.56 MHz) Ar/H_2 (4 %)/C_2H_2 plasmas is presented. The carbon nanospheres exhibit an amorphous structure being clearly observed at 0.1 Torr, 300 W and growing in size with increasing C_2H_2 between 1 % and 20 %. Above a C_2H_2 concentration threshold (20 % in our case) no carbon nanoparticles are formed anymore. In order to study possible changes in the plasma kinetics, optical emission spectroscopy (OES) is used to evaluate the electron temperature while changing the C_2H_2 concentration. In addition, an analysis of the temporal evolution of the electron energy distribution function (EEDF) is carried out for different C_2H_2 concentrations considering the effects produced by electron-vibrational superelastic collisions and relative concentration of excited Ar atoms. Finally, the morphological and tribological features of the deposited films are characterized.

1. Introduction

Plasma enhanced chemical vapour deposition (PECVD) at relatively low pressures is nowadays used for fabricating carbon-based nanostructures such us, for instance, carbon nanoparticles and ultrananocrystalline diamond using reactive hydrocarbon/argon plasmas produced in different kind of microwave (MW) and radio-frequency (RF) discharges [1]. There is a certain range of conditions in methane and acetylene gas discharges in which dust particles have been detected in the plasma bulk [2]. As it is known, the incorporation of nanoparticles into growing films can be used to modify and somehow control the film properties.

We report here a study of the synthesis and morphological and tribological characterization of nanocarbon structures deposited with low pressure (0.1 Torr) C_2H_2/H_2 (4 %)/Ar plasmas produced in RF (13.56 MHz) capacitively coupled discharges with high excitation power (300 W) and changing the initial concentration of C_2H_2 (from 1 % to 20 %). The latter is accompanied with an analysis of the plasma using optical emission spectroscopy (OES) aimed to detect possible changes in the excited species in the plasma during the production of carbon nanoparticles of larger size (from 50 nm to about 120 nm in diameter) while increasing the amount of C_2H_2.

On the other hand, we have also evaluated how the increasing concentration of C_2H_2 in the investigated RF discharges together with different values of the vibrational temperature and relative amount of excited argon atoms affect the electron energy distribution function (EEDF) and its temporal modulation. The results from such simulations will let us know not only the degree of temporal modulation but also how plausible it is to assume the commonly used Maxwellian shape. The analysis of the time modulation of the EEDF in low pressure RF-produced $C_2H_2/H_2/Ar$ plasmas has not been previously reported. Here we have linked the EEDF simulations with properties of the deposited films by using different values of electric fields associated with the range of particle diameters observed within the films.

2. Experimental set up

A parallel-plate aluminium reactor was used as deposition chamber. While the plasma is on (300 W), the chamber is pumped by a rotary vacuum pump resulting in a pressure of 0.1 Torr for typical flow rates of 74-95 sccm Ar, 4 sccm H_2 and 1-20 sccm C_2H_2. After each run, the chamber is cleaned using O_2 and is then pumped by a vacuum system (roots and rotatory pump). The gases are introduced through the upper electrode, which is of the showerhead type. The gas flow rates are controlled and monitored by mass flow controllers during the deposition process (120 min).

A RF generator (13.56 MHz) is capacitively coupled to the upper electrode through an impedance matching network with an allowed maximum reflected power of 10 W. The lower electrode is grounded. The electrodes are 30 cm in diameter and are separated by a 5 cm gap. The emission pattern resulting from the different emitting species in the plasma was detected by OES measurements using a monochromator with 0.275 m focal length, a

resolution of 0.1 nm, an entrance slit of 25 μm and a grating of 1200 grooves/mm. The emitted light from the studied plasmas was collected five minutes after the plasma was ignited using an unintensified 1024-pixel diode array detector 180-1100 nm (model 1453).

The thickness of the deposited samples has been measured by profilometry. The atomic composition of the samples has been analysed by Infrared (IR) spectroscopy and Electron Energy Lost Spectroscopy (EELS). The nanostructure of the deposit has been studied by scanning (SEM), transmission (TEM) electron and atomic force (AFM) microscopies. Finally, the tribological behaviour has been evaluated by undergoing the samples to nanoindentation and pin-on-disc tests.

The wear coefficient was calculated as the volume loss from the width and the depth of the wear track measured by profilometry. Wear was normalized to the distance covered by the tip and the applied load.

3. Results and discussion

3.1. Study of the plasma: OES and EEDF analysis

Carbon nanoparticles have been detected in carbon films deposited from Ar/H_2 (4 %)/C_2H_2 plasmas produced at 0.1 Torr and 300 W in a RF (13.56 MHz) discharge with 1 % (1 sccm of the total incoming gas flow) of C_2H_2. No particles are found if the pressure and/or the excitation power are changed or if the relative amount of argon is changed with respect to that of H_2 (keeping the relative concentration of C_2H_2 constant at 1 %). The increase up to 20 % (20 sccm) of the amount of C_2H_2 in the feed gases, keeping constant the initial concentration of H_2, produces the increase of the nanoparticle diameter (from ~ 50 nm to ~ 200 nm).

OES spectra, recorded 5 minutes after ignition of the plasma, shows that Ar lines are the most abundant and that the fact of using 20 sccm of C_2H_2 causes a decrease of Ar lines while no lines associated with C_2H_2, or its dissociation products, are visible.

Using a technique that we have developed in a previous work [3], the present OES data are used to evaluate the electron temperature of the plasma as a function of the content of C_2H_2. The temperatures obtained are shown in Table 1 where we can see that T_e remains fairly constant (within experimental error) when the concentration of C_2H_2 increases.

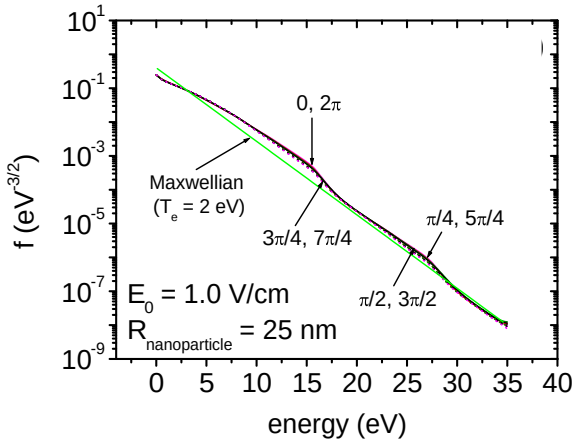

Figure 1. Time-dependent EEDF f(ε,t) in Ar(76 %)/H_2(4 %)/C_2H_2(1 %) after periodic steady state has been reached for Ar* (4s) = 10^{-2}×Ar and E_0 = 1.0 V cm^{-1} (E_0/N = 33 Td). In all cases we have used T_{vib} = 3000 K.

Since the method we have used to evaluate T_e assumes Maxwellian electron energy distribution function (EEDF), it is interesting to find out how reasonable it is this approach for the kind of plasmas we are dealing with.

Using the approach described in Ref. [4] and the electron kinetic processes reported in Ref. [5], we have solved the spatially uniform time-dependent Boltzmann equation with a sinusoidal electric field ($E = E_0 \sin(\omega t)$ with $\omega = 2\pi\nu$ and ν = 13.56 MHz with E_0 = 0.6 V cm^{-1} - 1.0 V cm^{-1}) to study the degree of temporal modulation of the EEDF that will allow us to know whether the DC effective field approximation and/or the use of a DC electric field of magnitude equal to that of the actual RF field at the corresponding instant in time (the quasi-steady-state (QSS) approximation) are applicable. The value of the amplitude E_0 of the electric field is chosen following recent results on predicted values of the electric field in dusty plasmas as a function of the dust particle size [6].

We have chosen two limit values of E_0 equal to 0.60 V/cm and 1 V/cm in the plasma bulk which, according to recent results by Denysenko *et al.* [6] for conditions quite similar to ours, are related to particle diameters of 50 nm (1 % C_2H_2) and 200 nm, (20 % C_2H_2). In addition, other results by Denysenko *et al.* [7] have shown that, for relatively high dust density (~ 5×10^7 cm^{-3}) and/or dust radius (~ 100 nm), the solutions of the uniform Boltzmann equation are reasonable to describe the effect of plasma nonuniformity on the EEDF.

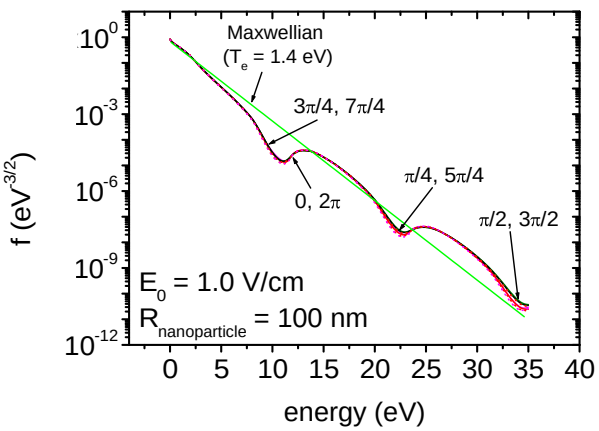

Figure 2. Time-dependent EEDF f(ε,t) in Ar(76 %)/H_2(4 %)/C_2H_2(20 %) after periodic steady state has been reached for Ar* (4s) = 10^{-2}×Ar and E_0 = 1.0 V cm^{-1} (E_0/N = 33 Td). In all cases we have used T_{vib} = 3000 K.

Figures 1 and 2 show the EEDF for the same E_0 but changing the amount of C_2H_2 (associated with different particle size).

Table 1: Comparison of electron temperatures obtained from measurements (T_e ± 10 %), Maxwellian fits and the magnitude 2/3 <ε> obtained from the steady state solution of the homogeneous Boltzmann equation for different C_2H_2 concentrations (and nanoparticle radius as seen by SEM) in the case of Ar* = 0.01×Ar

C_2H_2 (%)	$R_{Particle}$ (nm)	E_0 (V/cm)	T_e^{Exp} (eV)	T_e^{Max} (eV)	2/3 <ε> (eV)
20	100	1.00	1.35	1.40	1.15
10	60	0.85	1.34	1.50	1.28
1	25	1.00	1.37	2.00	2.60
1	25	0.75	1.37	2.00	2.20
1	25	0.60	1.37	1.90	2.05

We have also considered the impact on the EEDF of different concentrations (relative to ground state) of excited Ar states and of two values (3000 K and 300 K) of the vibrational temperature so that the possible effects produced by electron-vibrational superelastic collisions are included.

Keeping fixed the concentration of C_2H_2 (1 % or 20 %), the increase from 10^{-4} to 10^{-2} of the fraction of excited Ar atoms is also responsible of a lower modulation of the EEDF. We did not find significant differences when using T_{vib} = 300 K or T_{vib} = 3000 K. However, T_{vib} = 3000 K was used for consistency with recent measurements of the vibrational temperature in DC and RF produced H_2 plasmas.

Together with the calculated EEDFs, we have also included in Fig. 1 and Fig. 2 the best possible Maxwellian fits. It can clearly be seen that, an increase of the amount of C_2H_2 (keeping Ar* and E_0 constant) up to 20 % produces a Maxwellization of the calculated EEDF (see T_e^{Exp} vs <ε> in Table 1). However, a Maxwellization of the EEDF is also produced when E_0 is adapted to the particle size (see in Table 1 the case of $R_{Particle}$ = 25 nm with 0.6 V/cm instead of using 1 V/cm). It is worth mentioning that, in reasonable agreement with measurements of T_e with increasing C_2H_2, the values of the T_e associated with the Maxwellian fits (better for 20 % C_2H_2) exhibit a decreasing trend with growing C_2H_2.

As seen from Fig. 1 and Fig. 2, the assumption of a Maxwellian shape for the EEDF is, in general, better justified for high concentrations of C_2H_2 (see Table 1). Finally, due to the small time modulations of the EEDFs predicted for the cases of 1 % and 20 % of C_2H_2, the DC effective field approximation could be used when Ar* (4s) = 10^{-2} Ar and Ar* (4s) = 10^{-4} Ar.

3.2. Synthesis and characterization of films

Carbon films with embedded nanoparticles have been deposited by RF-PECVD from Ar/H_2/C_2H_2 mixtures varying the C_2H_2 content. As it can be seen in Fig. 3, the deposition rate of the film sharply increases with growing acetylene percentage because of the increase in the carbon precursor species present in the reactor. Further increment in the acetylene content (> 10 %) produces the formation of films which are promptly detached from the silicon substrate.

From the IR and EELS results, we concluded that the films consist in a carbon and hydrogen structure with most of the hydrogen atoms bounded to sp^3 carbon atoms (C-H vibration IR band below 2950 cm^{-1}). Moreover, the analysis of the infrared C-H band has allowed us to detect a slight decreasing trend for the hydrogen content as the acetylene content increases from 1 % to 10 %. On the other hand, no significant differences in the sp^2/sp^3 ratio (sp^2/sp^3 ~ 0.39), calculated from the EELS spectra of the films, have been found when increasing the amount of C_2H_2 in the gas mixture.

Nanoparticles have been detected in all the deposits, and their size (observed by SEM images) increases as the acetylene concentration in the plasma becomes higher (see Fig. 3). The increment in size goes in parallel with a change in the nanoparticle shape, that is, for low acetylene content (1 %) spherical nanoparticles, 40-50 nm in diameter, have been detected, whereas larger nanoclusters (80-120 nm) with slightly different shape have been observed, as higher acetylene concentrations are used.

The presence of nanoparticles in the films has been confirmed by AFM, indicating the increase of the particle diameter with increasing acetylene concentration.

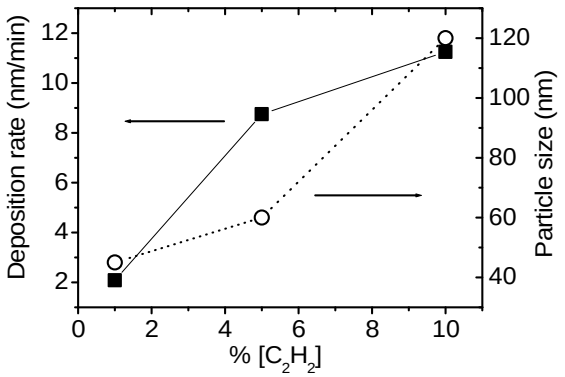

Figure 3. Deposition rate of carbon films and nanoparticle size (diameter) *vs* the acetylene content in the gas mixture

Furthermore, one can readily calculate, based on AFM images, the root mean square (rms) roughness. We have observed a linear increase from 3 nm to 8 nm of the film rms roughness with the diameter of the particles as determined from SEM images. Finally, the use of TEM revealed that the observed nanoparticles have an amorphous structure formed by several piled-up layers.

3.3. Tribological behaviour

In order to minimize the effect of the silicon substrate during nanoindentation tests, 1 μm thick carbon films with nanoparticles were prepared using different acetylene concentrations in the gas mixture. We detected an improvement in the hardness, calculated using the Oliver and Pharr method, of the coating with growing acetylene concentration and in coincidence with the increase in the diameter of the nanoparticles formed in the deposit. The variation of the hardness as a function of the nanoparticle goes from 3 GPa (1 % C_2H_2) to 10 GPa (10 % C_2H_2).

The friction coefficient of the deposited coatings was measured continuously during the test, showing low values (0.13 - 0.36 range) compared with the value of 0.6 obtained for uncoated silicon substrates. An improvement in the friction and wear behaviour of the coatings was detected as the nanoparticle size increases from 50 nm to 120 nm.

As pointed out by several authors, the presence of amorphous carbon nanoparticles embedded in the deposited thin films may account for the improvement in their tribological properties.

From the results presented, it may be deduced the hardening as well as the decrease in the friction and wear coefficients as the particle size increases.

4. Conclusions

The analysis of the EEDF of the RF-driven C_2H_2/H_2 (4 %)/Ar plasma shows that the temporal modulation of the electron distribution function is, in general, quite small. In addition, we found that, independently of the relative concentration of C_2H_2, the increase of excited argon atoms produces a further decrease of the EEDF time modulation. Finally, the EEDF becomes more Maxwellian with higher C_2H_2 (when keeping Ar* and E_0 constant) and, in reasonable agreement with measurements of T_e with increasing C_2H_2, the values of the T_e associated with the Maxwellian fits (better for 20 % C_2H_2) exhibit a decreasing trend.

Regarding the coating analysis, amorphous carbon films with carbon nanoparticles embedded have been deposited by RF-PECVD from acetylene/hydrogen/argon gas mixtures. Well-adhered coatings with the nanoparticle size increasing in the 50-120 nm range have been grown as the acetylene concentration varies from 1 % to 10 %. The increase in the nanoparticle size leads to an improvement in the tribological properties of the coatings, their hardening and reduction of the friction coefficient and the wear rate.

5. References

[1] S. Hong, J. Berndt, J. Winter, Plasma Sources Sci. & Technol. **12** (2003) 46.
[2] J. Berndt, S. Hong, E. Kovacevic, I. Stefanovic, J. Winter, Vacuum **71** (2003) 377.
[3] F. J. Gordillo-Vázquez, M. Camero, C. Gómez-Aleixandre, Plasma Sources Sci. & Technol. **15** (2006) 42.
[4] W. L. Morgan, Comp. Phys. Communications, **58** (1990) 127.
[5] M. Camero, F. J. Gordillo-Vázquez, C. Gómez-Aleixandre, CVD Journal (2007) (accepted).
[6] I. Denysenko, J. Berndt, E. Kovacevic, I. Stefanovic, V. Selenin, J. Winter, Phys. Plasmas, **13** (2006) 073507.
[7] I. Denysenko, M. Y. Yu, S. Xu, J. Phys. D: Appl. Phys. **38** (2005) 403.

Acknowledgements

F.J.G-V. acknowledges partial financial support from CSIC-CAM (Project No. 200650M016) and MEC (Projects No**.** MAT2006-13006-C02-01 and ENE2006-14577-C04-03). C.G-A. acknowledges partial financial support from MEC (Projects No**.** MAT2002-04085-02-02 and MAT2006-13006-C02-01). Both authors acknowledge partial support from "Fundación Domingo Martínez" (Project No. 4.2).